

Learning from SAM: Harnessing a Segmentation Foundation Model for Sim2Real Domain Adaptation through Regularization

Mayara E. Bonani*, Max Schwarz*, and Sven Behnke

Abstract—Domain adaptation is especially important for robotics applications, where target domain training data is usually scarce and annotations are costly to obtain. We present a method for self-supervised domain adaptation for the scenario where annotated source domain data (e.g. from synthetic generation) is available, but the target domain data is completely unannotated. Our method targets the semantic segmentation task and leverages a segmentation foundation model (Segment Anything Model) to obtain segment information on unannotated data. We take inspiration from recent advances in unsupervised local feature learning and propose an invariance-variance loss structure over the detected segments for regularizing feature representations in the target domain. Crucially, this loss structure and network architecture can handle overlapping segments and oversegmentation as produced by Segment Anything. We demonstrate the advantage of our method on the challenging YCB-Video and HomebrewedDB datasets and show that it outperforms prior work and, on YCB-Video, even a network trained with real annotations.

I. INTRODUCTION

Domain Adaptation is the art of transferring knowledge learned from one domain to another domain, usually the application domain. For roboticists in particular, the very idea of using out-of-domain data is very appealing, since target domain data is usually not available in quantities that are interesting for modern deep learning approaches, and target domain *annotations* are even more costly to obtain.

Synthetic data is one kind of out-of-domain data, which is particularly cheap to generate. It can get close to the target domain in many properties, but still suffers from *domain gap*, the effect that the data distributions do not overlap perfectly and thus a trained model cannot generalize from training domain to application domain. In the case of synthetic data, this is more specifically also called the *Sim2Real gap* [1].

While there is ongoing research on decreasing this gap through improvement of synthetic generators [2], [3] or learning to adapt training data to fit a target distribution [4], we choose to approach the issue from another, orthogonal direction: Can we regularize the model in a task-specific manner so that it performs more robustly in the target domain?

Recently, *foundation models*, i.e. very large models trained on internet-scale datasets, have been released for various tasks. One of these, the Segment Anything Model (SAM) [5] targets segmentation tasks and demonstrates impressive performance in prompted settings, i.e. where there is some knowledge of the target objects' location. Still, SAM is

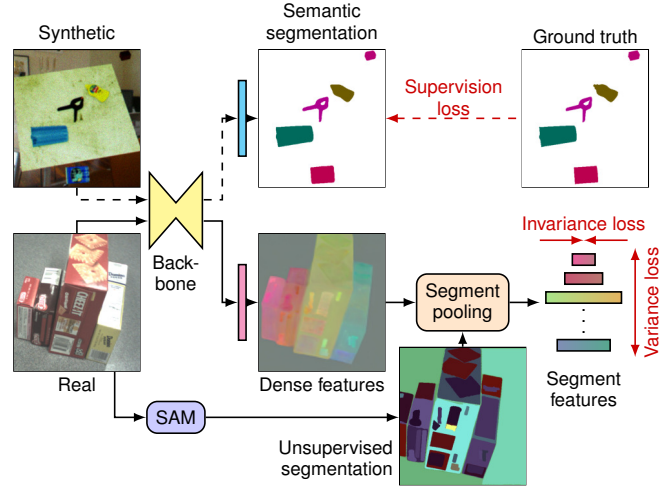


Fig. 1. Hybrid learning from annotated synthetic data (top path, dashed) and unannotated real data (bottom path, solid). For synthetic data, ground truth is available. For real data, projected dense features are aggregated using segment information obtained from Segment Anything Model (SAM). An invariance loss forces feature vectors of the same segment closer together, while a variance loss spreads segment means apart. Both branches of the network train the backbone and thus benefit from each other.

not suitable for most robotic applications as-is, since it does not have any knowledge of the target semantics (e.g. object classes) and is much to compute-intensive for real-time application.

In this work, we explore a way of distilling the general “objectness” knowledge learned by SAM and leveraging it to achieve robust domain adaptation of semantic segmentation networks. In particular, we use SAM to generate a regularization signal for the task model on unlabeled target domain data by pooling dense features into detected segments (see Fig. 1). We then use an invariance-variance loss scheme inspired by recent advancements in self-supervised feature learning [6], [7] to regularize the network’s learned features on unannotated real data.

This method yields results significantly outperforming a prior Sim2Real adaptation method [4]. It is even superior to models trained with real annotations.

Our contributions include:

- 1) an end-to-end pipeline for Sim2Real domain adaptation,
- 2) a segment pooling module which uses pre-extracted SAM segments to aggregate features,
- 3) a loss scheme that allows self-supervised learning on a combination of annotated synthetic data and unannotated real data, and

*Equal contribution.

All authors are with the Autonomous Intelligent Systems group of University of Bonn, Germany; schwarz@ais.uni-bonn.de

- 4) thorough evaluation on the challenging YCB-Video and HomebrewedDB datasets and two different synthetic data generators.

II. RELATED WORK

◦ *Synthetic Data*. Annotated data is difficult and costly to obtain, in particular for the large variety of applications in robotics. As an alternative, synthetic data generation is a very promising approach, since precisely-labeled training data can be generated cheaply. Schwarz and Behnke [2] introduce the Stilleben framework, which generates training data for perception tasks such as semantic segmentation, object detection, and pose estimation. The images provided by Stilleben are obtained through physics simulation of object meshes and rasterization, allowing the objects to have a randomized appearance and material parameters in addition to noise and transformations that simulate the camera sensors in a scene. Denninger *et al.* [3] propose BlenderProc, which also generates photo-realistic synthetic images. In contrast to Stilleben, its focus is on the realism of the resulting images, employing offline rendering techniques such as path tracing using the well-known Blender software. For this work, we use both Stilleben and BlenderProc in order to evaluate our method for different synthetic data generators.

◦ *Unsupervised Learning*. If only unlabeled data is available, one can also turn to unsupervised learning techniques to learn robust features on it. Joint embedding architectures represent one of the main streams in recent works. Bardes *et al.* [6] proposed a self-supervised method for training such architectures, called Variance-Invariance-Covariance Regularization (VICReg). First, the variance regularization term is defined as a hinge function on the standard deviation of the embeddings along the batch dimension and above a given threshold. It thus forces the embedding vectors of samples within a batch to be different. Two augmentations of the same sample, in contrast, are forced closer together by the invariance term. Finally, the covariance term encourages decorrelated feature dimensions. Overall, the authors show that their regularization stabilizes training and leads to robust learned features.

The VICReg approach performs well for classification tasks, but it is not suitable for image segmentation because it removes spatial information to satisfy the invariance criterion. To address semantic segmentation tasks, the model needs to focus on learning local information. With this motivation, as a solution to consider global and local features simultaneously, the VICRegL method by Bardes *et al.* [7] learns at different scales. At the global level, the VICReg criterion is applied in the same way as before. At the local level, it uses spatial information to match feature vectors that are pooled from nearby regions in the original image (pixels that have a small distance between them) or by the smallest distance in the embedding space. The VICReg criterion is applied only to the top- γ l^2 nearest-neighbors (NN) feature vectors considering image locations and feature maps. Our loss structure is inspired by the VICReg criterion, but in contrast to VICRegL, our method leverages external

(over-)segmentation information generated by SAM to derive intra-frame correspondences. Another difference is that we employ a modern segmentation backbone architecture which is able to generate features in a much higher resolution.

Perhaps most related to our approach, Hénaff *et al.* [8] group local feature vectors according to a simple unsupervised pre-segmentation and apply a contrastive objective to each object-level feature separately. Their contrastive objective maximizes the similarity across views of local features which represent the same object while minimizing its similarity for local features from different objects. In contrast to their work, which focuses on self-supervised pretraining, our method makes use of the available supervision on synthetic data during training.

◦ *Domain Adaptation*. Although synthetic data is a viable solution to the annotation bottleneck problem, it suffers from the domain gap between synthetic and real data, i.e. the discrepancy between the statistical properties obtained by the synthetic data distribution and the real data distribution. To overcome the performance degradation when the model is trained using real images, Imbusch *et al.* [4] suggested a multi-step learning-based approach to perform synthetic-to-real domain adaptation and consequently minimize the domain gap. Similar to our work, synthetic images are generated using Stilleben [2]. The images are then fed into a domain adaptation network, which outputs images more similar to the real dataset while preserving annotations. This domain adaptation approach is based on Contrastive Unpaired Translation (CUT) [9], which is an image-to-image translation technique aimed at preserving the image content while adapting the appearance to the target domain. CUT is a GAN-based approach that uses a contrastive loss on image patches to achieve content preservation by ensuring that a patch of the translated image has more information in common with the same patch in the source image than with other patches from the source image. Instead of applying CUT to images at full resolution, Imbusch *et al.* [4] used a patch-based application of the CUT approach and improved the segmentation results obtained from synthetic data for two robotics datasets. Finally, the adapted images are used for training the task network. In contrast to this method, we do not adapt training images, but instead perform the adaptation while training the task network by regularizing its performance on unannotated data.

◦ *Segment Anything Model - SAM*. Foundation models (such as BERT [10], RoBERTa [11] and GPT-4 [12]) enable powerful generalization for tasks and data distributions beyond those seen during training. Kirillov *et al.* [5] focused on building a foundation model for image segmentation. The promptable segmentation task is to return a valid segmentation mask given any segmentation prompt, such as a set of foreground and background points or a rough bounding box specifying what to segment in an image. The Segment Anything Model (SAM) can adapt to diverse segmentation tasks. Importantly for a foundation model, the authors collected the Segment Anything Dataset, SA-1B, which consists of 11 million diverse, high-resolution, licensed, and privacy

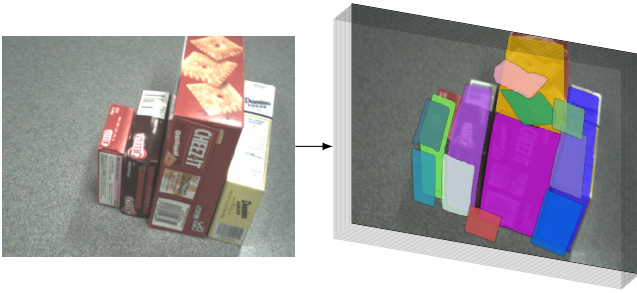


Fig. 2. Segments predicted by SAM in its “segment everything” mode, shown stacked in 3D on top of the reference image. Note how the segments overlap and over-segment the image. We only show a small number of segments for clarity.

protecting images and 1.1 billion high-quality segmentation masks. The dataset was collected through model-in-the-loop dataset annotation, leveraging weaker versions of SAM to annotate more training data for later stronger versions.

Although the model has some limitations, such as to miss fine structures, to segment small disconnected components, etc., the trained SAM model can segment unfamiliar objects and images without requiring any training or annotations and can be used for different tasks, as long as a prompt is available. SAM cannot be applied directly for usual semantic segmentation tasks, though, because it has no knowledge of the target classes. The produced segments can also intersect each other, making additional processing necessary to obtain only one label per pixel.

III. METHOD

We will now describe our method in detail. Fig. 1 shows the general information flow and Fig. 3 zooms into the trained network.

A. SAM Preprocessing

The Segment Anything Model (SAM, [5]) allows zero-shot segmentation given a point, mask, or even textual prompt. It has learned a general objectness concept which allows it to predict the most likely segment belonging to a prompt. We use the default “automatic” mask prediction mode of SAM, which queries the model with a grid of query points to segment “everything” in the image. The default settings are chosen for SAM with a ViT-H backbone. The number of points to be sampled along each side of the image is 24.

Because the SAM results only depend on the input image, SAM segmentation can be done in a preprocessing step. This is most welcome, since SAM execution is compute-intensive.

Because each segment is predicted in isolation, SAM produces an oversegmentation of the image with overlapping masks (see Fig. 2). To deal with this effect, we do not directly use the SAM segments to e.g. generate some pixel-wise pseudo labels, which would be difficult due to the overlapping. Instead, our chosen loss structure is able to deal with this ambiguity (see Sec. III-E).

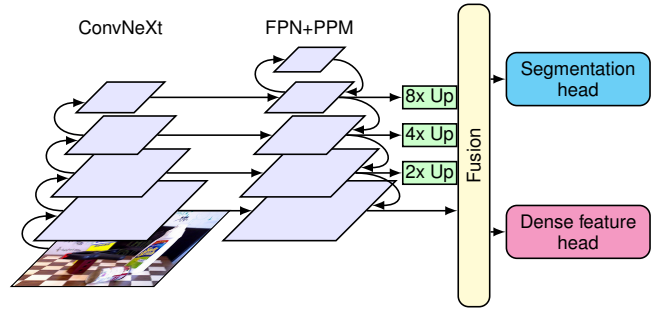


Fig. 3. Detailed architecture of the backbone with the segmentation and dense feature head. “Up” denotes a bilinear upsampling layer.

B. Modern Segmentation Backbone

The backbone of our network follows a standard architecture in recent segmentation works [13]–[15]: We combine a strong ConvNeXt-L [15] pretrained on ImageNet classification with a Feature Pyramid Network (FPN) [16], which propagates highly semantic features from higher, low-resolution layers back to the lower, high-resolution layers (see Fig. 3). Inspired by Xiao *et al.* [13], we also add an additional Pyramid Pooling Module (PPM) [17] on top of the feature pyramid, which improves global context by even further spatially aggregating features. A single fusion layer then produces a single feature map with 512 channels and high resolution. The resulting structure is similar to the one evaluated in [15] for segmentation tasks. Congruent with ConvNeXt, all our network layers use GELU activations.

C. Segmentation Head

A single convolutional layer with kernel size 1×1 computes the semantic segmentation result (i.e. class logits). On synthetic images, where annotations are available, this layer and the backbone are trained using the standard cross entropy loss

$$\mathcal{L}_{\text{Sup}} = \frac{1}{|I|} \sum_{p \in I} -\log \frac{\exp(x_{p,y_p})}{\sum_{c=1}^C \exp(x_{p,c})}, \quad (1)$$

where $p \in I$ are the pixels of the current frame, $x_{p,c}$ the logit prediction on pixel p for class $c \in C$, and y_p the ground truth class for pixel p .

For images without annotations, this output provides a compatible semantic segmentation but is not used for training.

D. Dense Feature Head

Inspired by VICReg [6] and VICRegL [7], we add a projection block for the self-supervised feature learning on real images. This projection block consists of two layers that bring the feature dimension first down to 256 and then to D . In our experiments we choose $D = 3$, which has the advantage of being easily visualizable as RGB colors. Low dimensionality in contrastively learned features are a common choice [18] and indeed, we did not observe higher performance in initial experiments with higher D .

The fact that the self-supervised feature learning uses a different projector than the semantic segmentation provides

the necessary decoupling: Since SAM oversegments the image, it is important that the segmentation head can ignore some fine-grained differences visible in the dense feature output (see the exemplary SAM output in Fig. 2).

E. Segment Pooling

Our way to use the SAM annotations is to pool together features that belong to the same segments as detected by SAM. In Hénaff *et al.* [8], for instance, the feature vectors coming from the same region in the mask are jointly pooled and the resulting vectors are contrasted between each other with a contrastive loss function. This allows feature vectors spatially far away in the original image to be pooled together if they belong to the same object. Following the same idea, we use the SAM segments to pool together regions in the feature maps.

After upsampling the output of the dense feature head to the image resolution, our pooling block computes the mean $\mu_i \in \mathbb{R}^D$ and the unnormalized variance vector $v_i \in \mathbb{R}^D$ for each segment $i \in \{0, \dots, N\}$:

$$\mu_i = \frac{1}{|S_i|} \sum_{p \in S_i} z_p, \text{ and} \quad (2)$$

$$v_i = \sum_{p \in S_i} (z_p - \mu_i)^{\odot 2}, \quad (3)$$

where S_i is the set of pixels belonging to segment i , z_p is the feature vector located at p , and $(\cdot)^{\odot 2}$ denotes the element-wise squaring operation (Hadamard power). The variance is not normalized by pixel count, since this would give equal importance to segments of any size, resulting in an undesired focus on smaller segments. Instead, we give each pixel of each segment equal weighting (see below).

Invariance Loss. The first information we can obtain from SAM is that pixels from the same segment are likely to belong to the same object. Thus, we strive to keep segment variance low. Therefore, we define the invariance loss

$$\mathcal{L}_{\text{Inv}} = \frac{\frac{1}{D} \sum_{i=1}^N \|v_i\|_1}{\sum_{i=1}^N |S_i|}. \quad (4)$$

Variance Loss. The second insight is that two different SAM segments are likely from different objects. We thus expect a minimum margin β between means, leading to the variance loss

$$\mathcal{L}_{\text{Var}} = \frac{2}{N(N-1)} \sum_{i \neq j} \max(0, \beta - \|\mu_i - \mu_j\|_2), \quad (5)$$

where we choose $\beta = 0.5$ as in [6].

We note that the assumption behind Eq. (5) does not hold in two cases: 1) Overlapping segments. In that case, variance and invariance loss will both be applied to the same pixels. In the end, this results in a balanced result, yielding the part-subpart observations made in Section IV-D. 2) Segments that do not intersect, but belong to the same object. In that case, SAM gave us no indication that the two segments belong to each other and we have to assume they are separate. We note that the segmentation head can learn to ignore this case through the synthetic supervision.

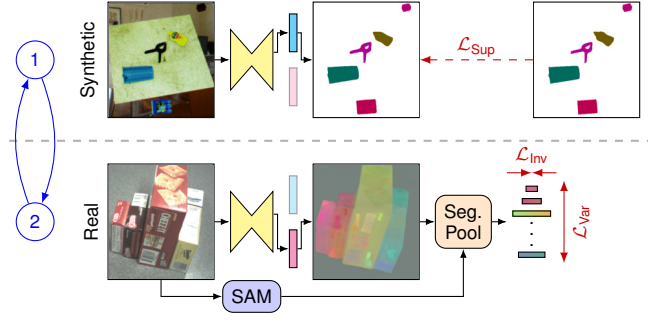


Fig. 4. Alternating training of the backbone and heads on synthetic (top) and real (bottom) data.

Bardes *et al.* [6] also propose a covariance loss which helps to keep individual feature dimensions decorrelated. In our experiments, we found that this component is unnecessary in our case, most likely because of the presence of supervision on synthetic images, which yields features (before the heads) that correspond to object classes.

The total loss in the self-supervised case on real images is thus

$$\mathcal{L}_{\text{real}} = \alpha (\mathcal{L}_{\text{Inv}} + \mathcal{L}_{\text{Var}}), \quad (6)$$

where $\alpha = 0.05$ is used to scale the loss in relation to the supervised loss on synthetic images, bringing them approximately to the same magnitude on the YCB-Video dataset.

IV. EVALUATION

A. Training Details

We follow the training and evaluation protocol of our prior work [2], [4]: Training is conducted over 300 epochs of 1500 frames each with a batch size of 1. Synthetic data is either generated on the fly (so that a frame is never repeated) or selected randomly from available frames. Accordingly, for real data the 1500 frames are randomly chosen from the entire dataset for each epoch. Similar to [4], an exponential moving average (EMA) version of the model is used for evaluation. We report the mean intersection over union (mIoU) score on the test dataset, averaged over the last 50 training epochs, which eliminates any remaining short-term training effects (see [4] for details).

Our full model requires both synthetic and real images. To keep RAM usage low, we follow an alternating training scheme (see Fig. 4), where in each iteration first a synthetic image is processed and then a real image. The supervised and self-supervised losses are thus only added stochastically over the course of optimization. Training was conducted on NVIDIA RTX A6000 and A100 GPUs.

B. Datasets

As in [4], we evaluate our method on the YCB-Video [19] and HomebrewedDB [20] datasets. Both datasets are part of the well-known BOP challenge [21] and contain object meshes—a prerequisite for generating synthetic data.

YCB-Video contains 21 YCB [22] objects captured with an RGB-D camera in 92 videos, totaling approx. 134k

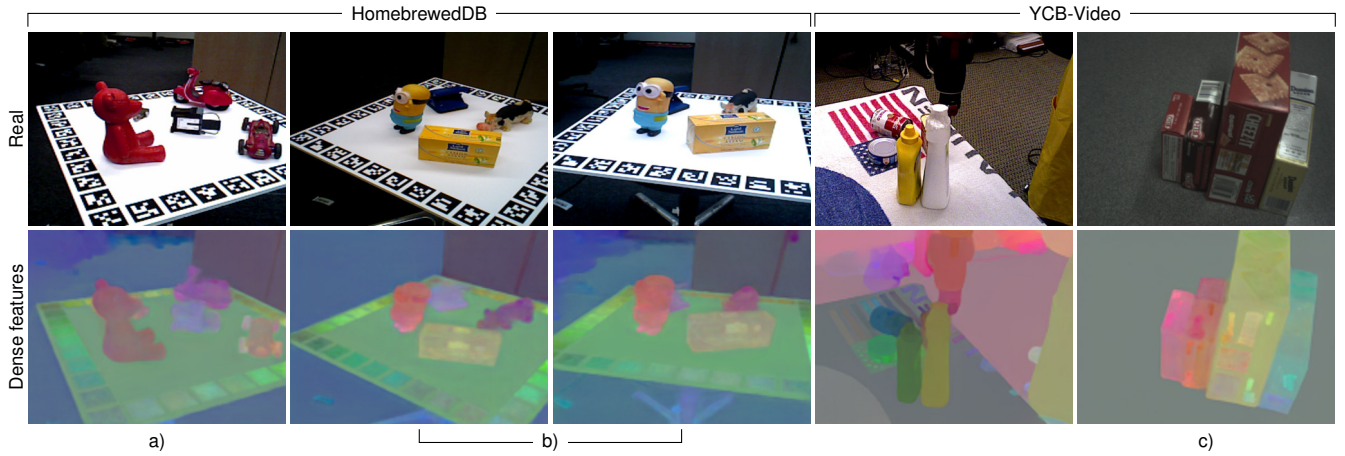


Fig. 5. Learned dense features normalized and visualized as RGB colors. The upper row shows input images from HomebrewedDB (left) and YCB-Video (right). The bottom row shows features learned by the network in self-supervised fashion. Note that a) features correspond well to objects, b) features are stable under camera motion, and c) SAM oversegmentation leads to sub-parts such as text receiving slightly different but related locations in feature space.

frames. The frames exhibit difficult lighting conditions and camera noise. For synthetic data, we use our prior work Stillleben [2], which generates physically plausible arrangements and renderings on the fly during training.

HomebrewedDB is a slightly smaller dataset with 13 different scenes. Following [4], we only use the Primesense frames. The “val” split is used for training, and the “test” split for evaluation (HomebrewedDB does not contain a “train” split with real data). The semantic segmentation is trained and evaluated only on the BOP test objects. For synthetic data, we use the BlenderProc4BOP synthetic frames provided by BOP. In earlier work [4] we used Stillleben data, but since Stillleben is not well adapted to HomebrewedDB, which contains many occluding background objects, we observed lower performance. The BlenderProc4BOP images allow us to demonstrate our method on a second type of synthetic data.

C. IoU Metric

To stay comparable with prior work [2], [4], we evaluate our models using the mean intersection over union metric, which is defined as follows:

$$\text{IoU}_c(I) = \frac{|P_c(I) \cap G_c(I)|}{|P_c(I) \cup G_c(I)|}, \quad (7)$$

$$\text{mIoU} = \frac{1}{|\mathbf{I}|} \sum_{I \in \mathbf{I}} \frac{1}{|C_I|} \sum_{c \in C_I} \text{IoU}_c(I), \quad (8)$$

where $P_c(I)$ are the pixels predicted for a particular class c on image I , $G_c(I)$ is the corresponding ground truth, C_I are the classes present in frame I , and \mathbf{I} is the set of test images.

D. Results

Table I reports quantitative results on YCB-Video and HomebrewedDB. We compare our results with those of Imbusch *et al.* [4], since they address the same problem setting. Similar to their evaluation, is not our intention to beat the overall state-of-the-art in semantic segmentation, but

TABLE I
RESULTS

Method	Mean IoU	
	YCB-Video [19]	HomebrewedDB [20]
Imbusch <i>et al.</i> [4]		
- real labels	0.770	0.737
- synthetic only	0.701	0.481 ¹
- full	0.763	0.558 ¹
Ours		
- real labels	0.839	0.883
- synthetic only	0.807	0.748
- CUT [4] only ²	0.814	-
- full	0.853	0.787 ³

Note: “real labels” is a baseline which has access to real supervision.

¹ Using Stillleben [2] synthetic data, where we use BlenderProc4BOP.

² Training our backbone on CUT-refined synthetic data.

³ Model was trained for only 200k epochs.

instead show the improvement gained by using our method when applied to a straightforward segmentation model.

As a first observation, our more modern segmentation backbone based on ConvNeXt and FPN+PPM compared to the older RefineNet [23] used in [4] is able to achieve much higher results on the baseline of real annotated data for both datasets. To analyze the impact of this further, we train an ablation of our backbone with CUT-refined data, like in [4]. This combination achieves similar results as compared to training our backbone directly on synthetic data. In conclusion, the more modern backbone architecture already provides the robustness that was induced through data augmentation in [4].

Furthermore, our method not only outperforms a network purely trained on synthetic data, but also manages to beat the real baseline on YCB-Video. On HomebrewedDB our method provides a decent advantage over synthetic data alone, but does not reach the performance possible from real annotations. This may be due to the smaller quantity and especially the smaller diversity of available real data.

Figure 5 shows the learned dense features qualitatively.

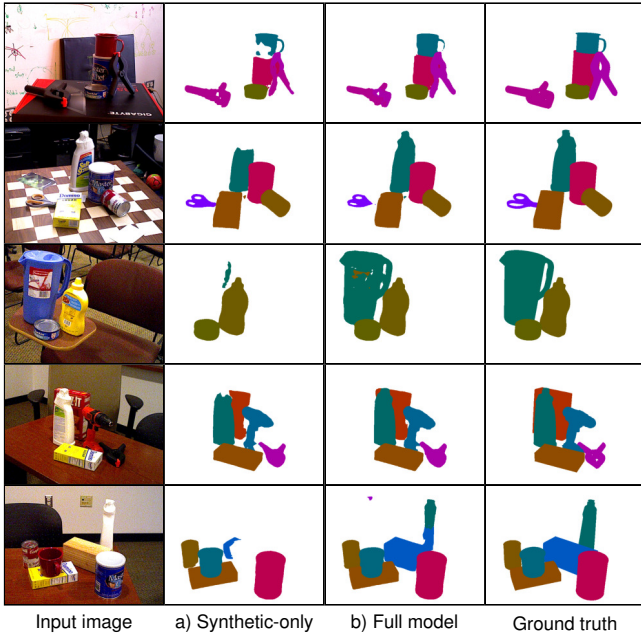


Fig. 6. Qualitative segmentation results on the YCB-Video test set. Compared to a model trained only on synthetic data a), the predictions of the model trained with SAM regularization b) are generally more complete.

It is immediately evident that the learned features correspond well to the objects to be segmented and it can be concluded that learning such a representation is highly likely to be helpful for the segmentation task. The fact that the learned representations remain stable under camera motion is a further indicator that the network is learning a shared representation for segmentation and dense features—since the invariance-variance loss alone does not demand such coherence. Interestingly, the feature visualizations exhibit the over-segmentation done by SAM. Small sub-parts of objects, such as text and/or markings receive slightly different feature values in order to satisfy the variance loss. Still, through the decoupled two-head design, this does not impact segmentation performance.

If we analyze the regularizing effect of SAM on the segmentation output, we can see that using the full pipeline encourages more complete segments (see Figs. 6 and 7). In contrast, a model trained only on synthetic data will often only detect parts of objects. In our opinion, this means that the general sense of “objectness” learned by SAM has been successfully distilled and combined with the target domain semantics by our approach.

Executing our model requires only one forward pass and is possible in real-time on an NVIDIA RTX A6000 GPU (40 ms per 640×480 frame). In contrast, the SAM backbone with grid prompting takes more than one second to process the same frame.

V. CONCLUSION

We demonstrated a practical way to address the annotation bottleneck by using source domain data with annotations and target domain data without annotations, leveraging and

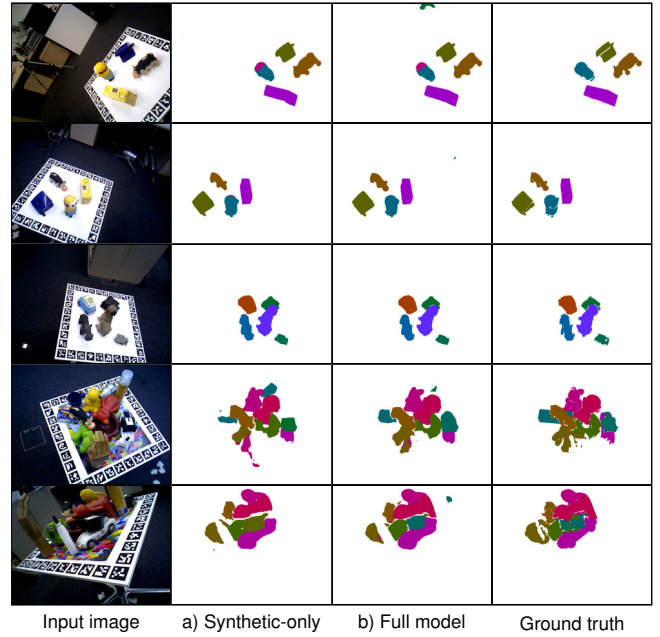


Fig. 7. Qualitative segmentation results on the HomebrewedDB test set. Compared to a model trained only on synthetic data a), the predictions of the model trained with SAM regularization b) are generally more complete.

learning from a foundation model.

Instead of focusing on improving the quality of the synthetic images, we make use of both domains to achieve a decrease in the Sim2Real gap. Indeed, we have shown that a task-specific regularization using a related foundation model is possible and beneficial for the task itself. Our method is universally applicable and we demonstrated its advantages for semantic segmentation on two well-known datasets. The evaluation of our method resulted in a mean IoU of 85% and 79% on YCB-Video and HomebrewedDB, a sufficient accuracy for real-world semantic tasks such as grasping.

Furthermore, the regularization term related to the SAM segments results in learning of meaningful features, which yields the observed improvement in task scores. At least on YCB-Video, our model trained only on synthetic data and SAM regularization can outperform models trained on real data. Therefore, we can regularize the model in a task-specific manner so that it performs more robustly in the target domain.

We believe the method is thus one quite generic tool roboticists can use to reduce the effects of the Sim2Real gap. We are convinced that our method will be applicable to other tasks than semantic segmentation, such as object detection, panoptic segmentation, 6D pose prediction, and other tasks requiring dense features.

ACKNOWLEDGMENT

This research has been funded by the Federal Ministry of Education and Research of Germany and the state of North-Rhine Westphalia as part of the Lamarr-Institute for Machine Learning and Artificial Intelligence.

REFERENCES

- [1] S. Höfer, K. Bekris, A. Handa, J. C. Gamboa, M. Mozifian, F. Golemo, C. Atkeson, D. Fox, K. Goldberg, J. Leonard, *et al.*, “Sim2Real in robotics and automation: Applications and challenges,” *IEEE Transactions on Automation Science and Engineering*, vol. 18, no. 2, pp. 398–400, 2021.
- [2] M. Schwarz and S. Behnke, “Stillleben: Realistic scene synthesis for deep learning in robotics,” in *IEEE International Conference on Robotics and Automation (ICRA)*, 2020, pp. 10 502–10 508.
- [3] M. Denninger, M. Sundermeyer, D. Winkelbauer, D. Olefir, T. Hodan, Y. Zidan, M. Elbadrawy, M. Knauer, H. Katam, and A. Lodhi, “BlenderProc: Reducing the reality gap with photorealistic rendering,” in *International Conference on Robotics: Scienc and Systems (RSS)*, 2020.
- [4] B. T. Imbusch, M. Schwarz, and S. Behnke, “Synthetic-to-real domain adaptation using contrastive unpaired translation,” in *18th IEEE International Conference on Automation Science and Engineering (CASE)*, 2022, pp. 595–602.
- [5] A. Kirillov, E. Mintun, N. Ravi, H. Mao, C. Rolland, L. Gustafson, T. Xiao, S. Whitehead, A. C. Berg, W.-Y. Lo, *et al.*, “Segment anything,” *arXiv preprint arXiv:2304.02643*, 2023.
- [6] A. Bardes, J. Ponce, and Y. Lecun, “VICReg: Variance-invariance-covariance regularization for self-supervised learning,” in *International Conference on Learning Representations (ICLR)*, 2022.
- [7] A. Bardes, J. Ponce, and Y. LeCun, “VICRegL: Self-supervised learning of local visual features,” *Advances in Neural Information Processing Systems (NeurIPS)*, vol. 35, pp. 8799–8810, 2022.
- [8] O. J. Hénaff, S. Koppula, J.-B. Alayrac, A. Van den Oord, O. Vinyals, and J. Carreira, “Efficient visual pretraining with contrastive detection,” in *International Conference on Computer Vision (CVPR)*, 2021, pp. 10 086–10 096.
- [9] T. Park, A. A. Efros, R. Zhang, and J.-Y. Zhu, “Contrastive learning for unpaired image-to-image translation,” in *European Conference on Computer Vision (ECCV)*, Springer, 2020, pp. 319–345.
- [10] J. Devlin, M.-W. Chang, K. Lee, and K. Toutanova, “BERT: pre-training of deep bidirectional transformers for language understanding,” in *Conference of the North American Chapter of the Association for Computational Linguistics: Human Language Technologies (NAACL-HLT)*, Association for Computational Linguistics, 2019, pp. 4171–4186.
- [11] Y. Liu, M. Ott, N. Goyal, J. Du, M. Joshi, D. Chen, O. Levy, M. Lewis, L. Zettlemoyer, and V. Stoyanov, “RoBERTa: A robustly optimized BERT pretraining approach,” *arXiv preprint arXiv:1907.11692*, 2019.
- [12] OpenAI, “GPT-4 technical report,” *arXiv preprint arXiv:2303.08774*, 2023.
- [13] T. Xiao, Y. Liu, B. Zhou, Y. Jiang, and J. Sun, “Unified perceptual parsing for scene understanding,” in *European Conference on Computer Vision (ECCV)*, 2018, pp. 418–434.
- [14] A. Kirillov, R. Girshick, K. He, and P. Dollár, “Panoptic feature pyramid networks,” in *Conference on Computer Vision and Pattern Recognition (CVPR)*, 2019, pp. 6399–6408.
- [15] Z. Liu, H. Mao, C.-Y. Wu, C. Feichtenhofer, T. Darrell, and S. Xie, “A ConvNet for the 2020s,” in *Conference on Computer Vision and Pattern Recognition (CVPR)*, 2022, pp. 11 976–11 986.
- [16] T.-Y. Lin, P. Dollár, R. Girshick, K. He, B. Hariharan, and S. Belongie, “Feature pyramid networks for object detection,” in *Conference on computer vision and pattern recognition (CVPR)*, 2017, pp. 2117–2125.
- [17] H. Zhao, J. Shi, X. Qi, X. Wang, and J. Jia, “Pyramid scene parsing network,” in *Conference on Computer Vision and Pattern Recognition (CVPR)*, 2017, pp. 2881–2890.
- [18] P. R. Florence, L. Manuelli, and R. Tedrake, “Dense object nets: Learning dense visual object descriptors by and for robotic manipulation,” in *Conference on Robot Learning*, PMLR, 2018, pp. 373–385.
- [19] Y. Xiang, T. Schmidt, V. Narayanan, and D. Fox, “PoseCNN: A convolutional neural network for 6D object pose estimation in cluttered scenes,” *Robotics: Science and Systems (RSS)*, 2018.
- [20] R. Kaskman, S. Zakharov, I. Shugurov, and S. Ilic, “HomebrewedDB: RGB-D dataset for 6D pose estimation of 3D objects,” in *International Conference on Computer Vision Workshops (CVPR)*, 2019.
- [21] M. Sundermeyer, T. Hodaň, Y. Labbe, G. Wang, E. Brachmann, B. Drost, C. Rother, and J. Matas, “BOP challenge 2022 on detection, segmentation and pose estimation of specific rigid objects,” in *Conference on Computer Vision and Pattern Recognition (CVPR)*, 2023, pp. 2784–2793.
- [22] B. Calli, A. Singh, A. Walsman, S. Srinivasa, P. Abbeel, and A. M. Dollar, “The YCB object and model set: Towards common benchmarks for manipulation research,” in *International Conference on Advanced Robotics (ICAR)*, 2015, pp. 510–517.
- [23] G. Lin, A. Milan, C. Shen, and I. Reid, “RefineNet: Multi-path refinement networks for high-resolution semantic segmentation,” in *Conference on Computer Vision and Pattern Recognition (CVPR)*, 2017, pp. 1925–1934.